Research Article | Vol. 31, No. 15 / 17 Jul 2023 / Optics Express 25082
Optics EXPRESS

Ab initio spatial phase retrieval via intensity triple correlations

NOLAN PEARD,[1,2] KARTIK AYYER,[3,4] AND HENRY N. CHAPMAN[2,4,5,6,*]

[1]Department of Applied Physics, Stanford University, Stanford, CA, USA
[2]Center for Free-Electron Laser Science CFEL, Deutsches Elektronen-Synchrotron DESY, Notkestr. 85, 22607 Hamburg, Germany
[3]Max Planck Institute for the Structure and Dynamics of Matter, 22761 Hamburg, Germany
[4]The Hamburg Center for Ultrafast Imaging, Universität Hamburg, Luruper Chausee 149, 22761 Hamburg, Germany
[5]Department of Physics, Universität Hamburg, Luruper Chausee 149, 22761 Hamburg, Germany
[6]Department of Physics and Astronomy, Uppsala University, Box 516, Uppsala SE-75120, Sweden
[*]henry.chapman@cfel.de

Abstract: Second-order intensity correlations from incoherent emitters can reveal the Fourier transform modulus of their spatial distribution, but retrieving the phase to enable completely general Fourier inversion to real space remains challenging. Phase retrieval via the third-order intensity correlations has relied on special emitter configurations which simplified an unaddressed sign problem in the computation. Without a complete treatment of this sign problem, the general case of retrieving the Fourier phase from a truly arbitrary configuration of emitters is not possible. In this paper, a general method for ab initio phase retrieval via the intensity triple correlations is described. Simulations demonstrate accurate phase retrieval for clusters of incoherent emitters which could be applied to imaging stars or fluorescent atoms and molecules. With this work, it is now finally tractable to perform Fourier inversion directly and reconstruct images of arbitrary arrays of independent emitters via far-field intensity correlations alone.

1. Introduction

Coherent diffractive imaging uses the stationary far-field interference of elastically-scattered light to infer the geometry of a scattering potential via Fourier analysis. Since most photodetectors perform an intensity measurement, information about the relative phases $\phi(\vec{m})$ of the scattered waves at pixels $\vec{m}$ is lost and Fourier inversion to real space is incomplete [1]. This "phase problem" is shared across a variety of imaging modalities, including x-ray crystallography and optical microscopy, and research in each field has arrived at a variety of techniques to obtain the phase information.

Non-stationary or incoherent scattering processes are known to provide more information, as much as twice the information cut-off in an optical microscope utilising incoherent illumination or fluorescence as compared with plane-wave illumination [2]. The far-field intensity distribution of such a process is featureless, but the measurement of intensity-intensity correlations can nevertheless be used to extract the Fourier amplitude of the object's structure as first demonstrated by Hanbury Brown and Twiss on the radio emission of bright stars [3]. This approach is attractive in situations where lenses of high enough angular or spatial resolution do not exist. This is certainly the case in the X-ray regime where recent work has examined the possibility of using photon pair correlations to retrieve the Fourier spectrum of x-ray fluorescence emission [4–9]. One is still left with the phase problem, which can be solved using iterative phase retrieval [9]

#495920 https://doi.org/10.1364/OE.495920
Journal © 2023 Received 22 May 2023; revised 29 Jun 2023; accepted 1 Jul 2023; published 13 Jul 2023

Optics EXPRESS

when the correlations are adequately and extensively sampled by detectors with large numbers of pixels. However, it has been known since the 1960s that intensity triple correlations can reveal partial phase information directly in the form of the so-called closure phase [10,11]. This has been heavily investigated in the field of radio astronomy [12–16] with the aim to develop the means to reconstruct an image of an arbitrary arrangement of emitters without the use of additional constraints.

Retrieval of the Fourier phase, $\phi(\vec{m})$, begins by first computing the absolute value of the *closure phase*, $\left|\Phi(\vec{m},\vec{n})\right| = \left|\phi(\vec{m}+\vec{n}) - \phi(\vec{m}) - \phi(\vec{n})\right|$, from the triple correlations. Unfortunately, we need the signed value of Φ to recover completely $\phi(\vec{m})$ for the following reason: At the start of phase extraction, an estimate value is chosen for the first pixel. But for the next pixel, the sign ambiguity of $|\Phi|$ returns two possible values of $\phi(\vec{m}+1)$ and an additional two possible values for every subsequent pixel (except for special arrays where $\mathrm{sgn}(\Phi)$ may be assumed constant). To avoid this exponential expansion of the solution space, we show how redundant information contained in $|\Phi|$ may be used to constrain the possible values of $\mathrm{sgn}(\Phi)$. Multiple publications have described the concept but, to the best of our knowledge, no one has yet provided complete or useful details on calculating $\mathrm{sgn}(\Phi(\vec{m},\vec{n}))$ [17–30]. Ab-initio phase retrieval from the third-order intensity correlations has thus remained incomplete for decades. With our method, it is now possible to solve for the phase of an arbitrary array of incoherent emitters from the third-order intensity correlations alone. Combined with the second-order intensity correlations, we have a completely general method for reconstructing images of arrays of incoherent emitters.

In this paper, we describe our solution to the sign problem of the closure phase, with the help of a simple 1D example using round numbers in section 3.1.1, and show a numerical implementation of our method with simulated data from classical independent light sources. This same method may be used to reconstruct images of star clusters or, with some corrections to account for the use of a quantum light source, arrays of fluorescent molecules or atoms.

2. Theory

The diagram in Fig. 1 depicts and contrasts structure determination via coherent scattering to that obtained from incoherent emission. When illuminated with a plane wave with a wave-vector $\vec{K}$, the elastically scattered field has stationary intensity given by

$$I(\vec{q}) = \left|\sum_{i}^{\nu} f_i e^{i\vec{q}\cdot\vec{r}_i}\right|^2 = \sum_{ij} f_i f_j^* e^{i\vec{q}\cdot(\vec{r}_i-\vec{r}_j)} \tag{1}$$

for a number ν of point scatterers with scattering factors f_i and positions $\vec{r}_i$ relative to an arbitrary real-space origin. The photon momentum transfer $\vec{q}$ is equal to the difference $\vec{k}-\vec{K}$. The phase of each scattered wave, $\vec{q}\cdot\vec{r}_i$, is derived from the difference in the optical path along the directions of the incoming and outgoing waves as compared to a scatterer at the origin. The intensity pattern is thus proportional to the square modulus of the Fourier transform $F(\vec{q})$ of the distribution of scatterers in terms of spatial frequencies equated with $\vec{q}$. The origin of the pattern, $\vec{q}=0$, is located in the direction of the incident beam. In this forward direction all scattered waves are in phase and there is strong constructive interference, with intensity generally falling with scattering angle. The pattern consists of speckles whose width is inversely proportional to the extent of the object. The recovery of the object's scattering potential is obtained by an inverse Fourier transform of $F(\vec{q})$, but only after the corresponding phases are obtained.

If, instead, the object consists of a collection of incoherent point emitters, then there is no dependence on any incident beam and the phase of the emission, relative to that of an emitter at an arbitrary real-space origin, is $\vec{k}\cdot\vec{r}_i + \phi_i$. We assume that the emission phases ϕ_i are random and uncorrelated on timescales greater than the relevant system coherence time, τ_c, due to

Optics EXPRESS

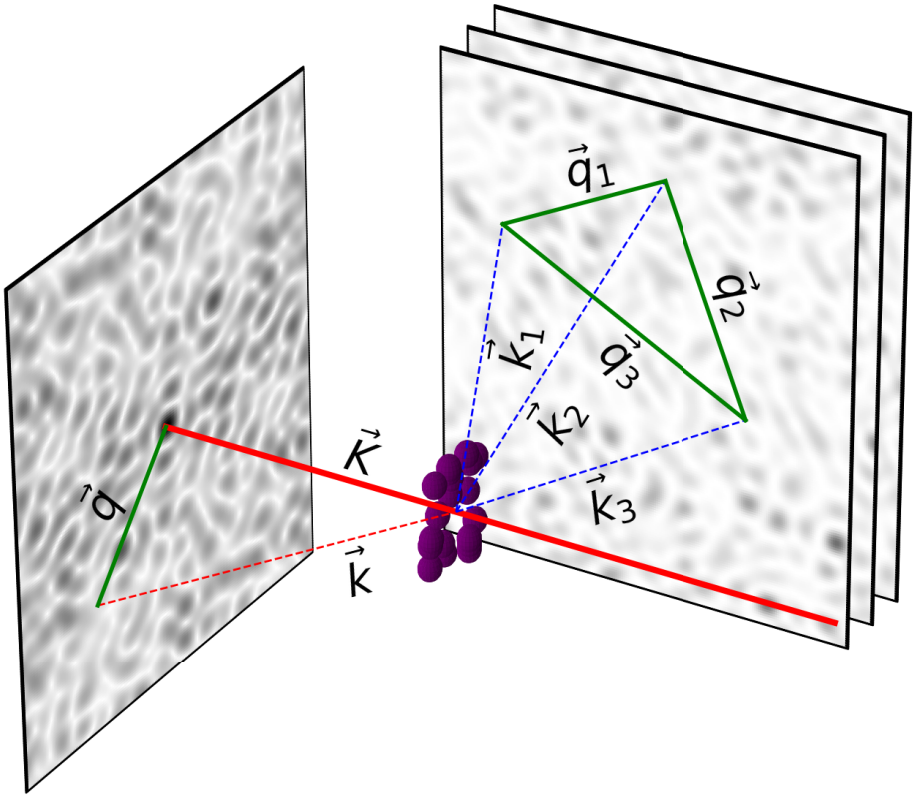

Fig. 1. Schematic of coherent diffraction in the forward detection plane, intersecting with the incident beam $\vec{K}$. Fluorescence speckle is emitted by the atoms isotropically and the position of the second detector is not dependent on the incident beam. Coherent diffraction data is collected as a function of the scattering vector $\vec{q} = \vec{k} - \vec{K}$. Correlations between triples of fluorescence photons (intensities) at pixels separated by $\vec{q}_1$, $\vec{q}_2$, and $\vec{q}_3$ reveal the spatial phase information lost in the coherent diffraction experiment.

independent, spontaneous emission at random times. The total light field in this scenario is often referred to as pseudo-thermal or chaotic and has intensity

$$I(\vec{k}) = \left| \sum_{i}^{\nu} s_i e^{i(\vec{k}\cdot\vec{r}_i + \phi_i(t>\tau_c))} \right|^2 = \sum_{ij} s_i s_j^* e^{i\left(\phi_i(t>\tau_c) - \phi_j(t>\tau_c)\right)} e^{i\vec{k}\cdot(\vec{r}_i - \vec{r}_j)} \tag{2}$$

with s_i the amplitude of electric field emission of the ith emitter. The intensity pattern depends on the orientation of the object, and, given the complete independence of emission, at an instant of time this pattern has a uniform intensity modulated by speckles of the same size as the case for coherent scattering. When rapid exposures are measured with a photodetector, we can consider the phases ϕ_i are reset shot-to-shot, changing the instantaneous speckle pattern. From the right-hand side of Eqn. (2), we observe that the structure (sum of $\vec{r}_i$ for all i) would be difficult to discern by averaging intensities over many shots—the random phase resets would drive the interference speckle visibility to zero. However, it remains possible to obtain structural information via intensity correlations [4].

In the following, we use the word *atom* to refer to any member of a collection of point fluorescent (atoms and molecules) or thermal (stars) light sources. We assume these atoms to

Optics EXPRESS

undergo spontaneous emission independently, i.e., that each atom emits a field with a phase or time delay that is uncorrelated to the fields emitted by the other atoms.

2.1. Intensity correlations

We consider photon emission vectors in reciprocal space, $\vec{k}_1$, $\vec{k}_2$, and $\vec{k}_3$, and their vector differences

$$\vec{q}_1 = \vec{k}_1 - \vec{k}_2 \tag{3}$$

$$\vec{q}_2 = \vec{k}_2 - \vec{k}_3 \tag{4}$$

$$\vec{q}_3 = \vec{k}_3 - \vec{k}_1 = -\vec{q}_1 - \vec{q}_2 \tag{5}$$

as depicted in Fig. 1. The ensemble average of third-order intensity correlations of the light field, Eqn. (2), over all shots

$$\left\{g^{(3)}(\vec{k}_1, \vec{k}_2, \vec{k}_3)\right\} = \left\{\frac{\langle I(\vec{k}_1)I(\vec{k}_2)I(\vec{k}_3)\rangle}{\langle I(\vec{k}_1)\rangle\langle I(\vec{k}_2)\rangle\langle I(\vec{k}_3)\rangle}\right\} \tag{6}$$

can be expressed as

$$\left\{g^{(3)}(\vec{q}_1, \vec{q}_2)\right\} \approx \left(1 - \frac{3}{\nu} + \frac{4}{\nu^2}\right) + \left(1 - \frac{2}{\nu}\right)\left(|g^{(1)}(\vec{q}_1)|^2 + |g^{(1)}(\vec{q}_2)|^2 + |g^{(1)}(-\vec{q}_1 - \vec{q}_2)|^2\right) \tag{7a}$$

$$+2\mathrm{Re}\left(g^{(1)}(\vec{q}_1) \quad g^{(1)}(\vec{q}_2) \quad g^{(1)}(-\vec{q}_1 - \vec{q}_2)\right) \tag{7b}$$

and is called the *bispectrum*. Similarly, the mean second-order intensity correlation function

$$\left\{g^{(2)}(\vec{k}_1, \vec{k}_2)\right\} = \left\{\frac{\langle I(\vec{k}_1)I(\vec{k}_2)\rangle}{\langle I(\vec{k}_1)\rangle\langle I(\vec{k}_2)\rangle}\right\} \tag{8}$$

may be written as

$$\left\{g^{(2)}(\vec{q}_1)\right\} \approx 1 - \frac{1}{\nu} + \left|g^{(1)}(\vec{q}_1)\right|^2 \tag{9}$$

where ν is the visibility. This equation is often referred to as the Siegert Relation in quantum optics [31]. For a full derivation of Eqs. (7) and (9) please review Supplement 1.

In Eq. (7), we have an expression for $g^{(3)}$ in terms of constants, the square modulus of $g^{(1)}$, and the real part of a product of complex-valued $g^{(1)}$. Since $\left|g^{(1)}\right|$ may be acquired from $g^{(2)}$ in Eq. (9), it is possible to extract the last term (7b) alone. This term is referred to as the *closure* in the astronomy literature. We can rewrite the *closure* as

$$\begin{aligned} &2\mathrm{Re}\left(g^{(1)}(\vec{q}_1) \quad g^{(1)}(\vec{q}_2) \quad g^{(1)}(-\vec{q}_1 - \vec{q}_2)\right) = \\ &\qquad 2\left|g^{(1)}(\vec{q}_1)\right|\left|g^{(1)}(\vec{q}_2)\right|\left|g^{(1)}(-\vec{q}_1 - \vec{q}_2)\right|\cos\left(\phi(\vec{q}_1) + \phi(\vec{q}_2) + \phi(-\vec{q}_1 - \vec{q}_2)\right) \end{aligned} \tag{10}$$

where we have expressed $g^{(1)}$ in polar coordinates in the complex plane. As the radial component ($\left|g^{(1)}\right|$) is easily obtained from $g^{(2)}$, the phase information, $\phi(\vec{q})$, can be isolated as follows.

Optics EXPRESS

Suppose we set $\vec{q}_1 = \vec{m}$ and $\vec{q}_2 = \vec{n}$ where $\vec{m}$, $\vec{n}$ map to discrete pixels on a detector. The symmetry of $\left|g^{(1)}(\vec{q})\right|$ and anti-symmetry of $\phi(\vec{q})$ allow us to rearrange the *closure* into

$$\cos\left(\phi(\vec{m}+\vec{n}) - \phi(\vec{m}) - \phi(\vec{n})\right) \approx \frac{g^{(3)}(\vec{m},\vec{n}) - (1 - \frac{3}{\nu} + \frac{4}{\nu^2}) - (1 - \frac{2}{\nu})(|g^{(1)}(\vec{m})|^2 + |g^{(1)}(\vec{n})|^2 + |g^{(1)}(\vec{m}+\vec{n})|^2)}{2\left|g^{(1)}(\vec{m})\right|\left|g^{(1)}(\vec{n})\right|\left|g^{(1)}(\vec{m}+\vec{n})\right|} \tag{11}$$

The inverse cosine of this expression is known as the *closure phase*, which we represent via the symbol

$$\Phi(\vec{m},\vec{n}) = \pm\left[\phi(\vec{m}+\vec{n}) - \phi(\vec{m}) - \phi(\vec{n})\right] \tag{12}$$

Just as in the Siegert Relation, the third-order correlation function encodes the phase $\phi(\vec{q})$ at pixels in $\vec{k}$-space beyond the physical spatial extent of the detector ($\left|\vec{q}_{\max}\right| = 2\left|\vec{k}_{\max}\right|$) as depicted in Fig. 1. Together, the double and triple correlations allow retrieval of the equivalent of a coherent diffraction pattern *and* its phase across an area of $\vec{k}$-space four times larger than the area of detector coverage [4,6].

3. Phase Retrieval

Equation (12) for the *closure phase* $\Phi(\vec{m},\vec{n})$ is a difference equation which can be used like a discrete derivative to estimate the slope of $\phi(\vec{m})$ between pixels separated by $\vec{n}$. The anti-symmetry of the phase pins $\phi(\vec{q} = \vec{0}) = 0$. Since overall translation in real-space results in phase ramps in reciprocal space, we can estimate the value of the phase at a nearest-neighbor pixel of

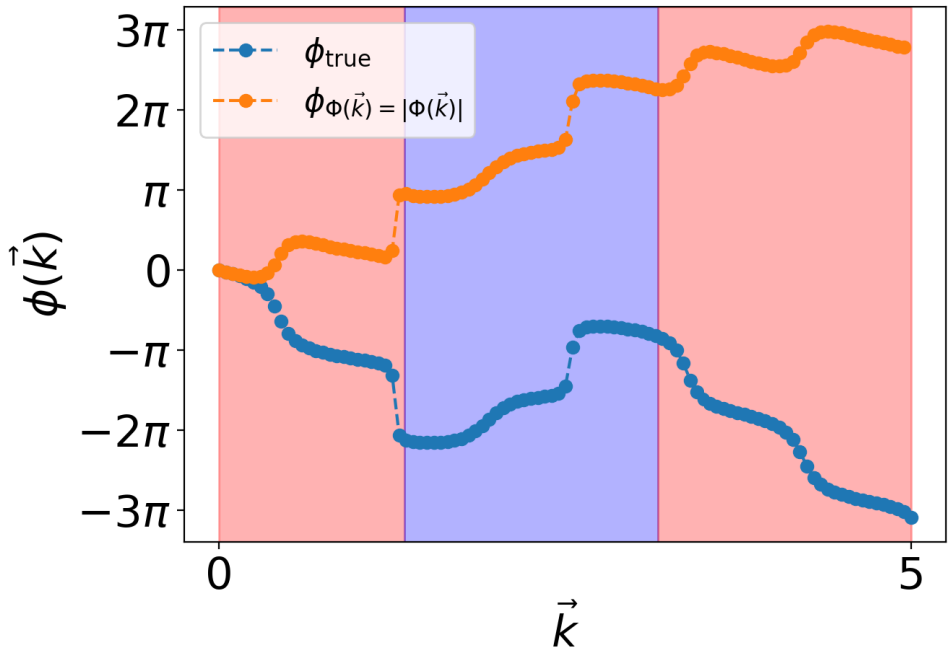

Fig. 2. Phase retrieved for a 1D detector assuming $\Phi(\vec{m},\vec{n}) = \left|\Phi(\vec{m},\vec{n})\right|$. The correct contour is recovered with the wrong slope in the sections highlighted in red. The blue highlight section has both the correct shape and slope, but is offset due to incorporation of incorrect ϕ early in the solution.

Optics EXPRESS

$\phi(\vec{q} = \vec{0}) = 0$ without loss of generality. This estimate can be refined later by seeking to minimize the total error (see Section 3.2) of all pixels and treating the initial value as a parameter. The difference equation and calculated $\Phi(\vec{m}, \vec{n})$ from experimental data reveals the value of the phase at the next-nearest-neighbor pixels and so forth until the phase on the entire pixel array has been calculated.

Once the second pixel of ϕ (next-nearest neighbor) in any direction is calculated, the interval of the difference equation ($\vec{n}$) may be increased to find the slope between every other (instead of every) pixel in the same direction. Essentially, the phase values calculated for pixels near the origin constrain the possible phase values of pixels far from the origin.

3.1. *Determining the sign of the closure phase sgn*(Φ)

Due to the sign ambiguity of the inverse cosine, every datum from $\Phi(\vec{m}, \vec{n})$ points to two possible values of the phase $\phi(\vec{m} + \vec{n})$

$$\phi(\vec{m} + \vec{n}) = +\Phi(\vec{m}, \vec{n}) + \phi(\vec{m}) + \phi(\vec{n}) \equiv \theta_+ \tag{13}$$

or

$$\phi(\vec{m} + \vec{n}) = -\Phi(\vec{m}, \vec{n}) + \phi(\vec{m}) + \phi(\vec{n}) \equiv \theta_- \tag{14}$$

for any $\vec{m}$ and $\vec{n}$. Assuming a global sign often leads to an incorrect slope for ϕ, as shown in Fig. 2. The fact that multiple values of $\Phi(\vec{m}, \vec{n})$ relate to the value of the phase at a single pixel allows us to determine the proper sign of $\Phi(\vec{m}, \vec{n})$ for each $\vec{m}$ and $\vec{n}$.

Suppose for a given pixel at $\vec{u}$ there exist N sets $(\vec{m}, \vec{n})$ in $\Phi(\vec{m}, \vec{n})$ for which $\vec{m} + \vec{n} = \vec{u}$. Each set offers a pair of possible values for $\phi(\vec{u})$, giving $2N$ possible values for $\phi(\vec{u})$ altogether. We know that each and every one of the N pairs contains the correct value, so comparing the N pairs should reveal it. Ideally, the correct value is included N times between the N pairs and is found simply by taking the intersection of all pairs. Next, we show a simple 1D example to illustrate the principle.

3.1.1. Phase retrieval 1D example

Suppose we have a $\phi(m) = (0, 1, -3, -1, 4, 2, 7)$ for $m = [0, 6]$. We can calculate a matching $\Phi(m, n)$ to which we add a sign ambiguity. (We will render our $\Phi(m, n)$ matrix with mn-axes such that the origin is in the bottom left corner, i.e., so that $\Phi(1, 1) = 5$).

$$|\Phi| = \begin{pmatrix} 0 & & & & & & \\ 0 & 4 & & & & & \\ 0 & 3 & 6 & & & & \\ 0 & 4 & 6 & 9 & & & \\ 0 & 1 & 10 & 6 & 6 & & \\ 0 & 5 & 1 & 4 & 3 & 4 & \\ 0 & 0 & 0 & 0 & 0 & 0 & 0 \end{pmatrix} \tag{15}$$

The upper right corner has no $m + n \leq 6$ and here the difference Eq. (12) is undefined.

Optics EXPRESS

For purposes of this demonstration, let us assume we have correctly estimated $\phi(1) = 1$. Then, we can try to determine $\phi(2)$ via

$$\Phi(1,1) = |\phi(2) - 2\phi(1)| = 5 \tag{16}$$

which gives the following options

$$\phi(2) = 5 + 2\phi(1) = 7 \tag{17}$$

or

$$\phi(2) = -5 + 2\phi(1) = -3 \tag{18}$$

Since this is a 1D example, there is no other point (m, n) such that we can deduce the correct value using $\Phi(m, n)$. The same is true for the calculation of $\phi(3)$ since we only have the information $\Phi(1, 2) = 1$ available to us. In a 2D phase retrieval we would have more values of Φ available to us to solve these pixels close to the origin, but for this 1D example, we will follow the branch we know to be correct with $\phi(2) = -3$ and $\phi(3) = -1$.

Now the core principle of our algorithm will be demonstrated. We want to find $\phi(4)$ using $\phi(1)$, $\phi(2)$, $\phi(3)$, $\Phi(2, 2)$, and $\Phi(1, 3)$. This is the first pixel for which we have two constraints on $\phi(4)$ via $\Phi(2, 2)$ and $\Phi(1, 3)$

$$\phi(4) = \pm\Phi(2,2) + 2\phi(2) = \pm 10 + -6 \tag{19}$$

$$\phi(4) = \pm\Phi(1,3) + \phi(1) + \phi(3) = \pm 4 + 0 \tag{20}$$

which gives us four possible values of $\phi(3)$ in two pairs labeled by the points on the Φ matrix that are associated with $(\Phi(2, 2) \rightarrow \{4, -16\}$ and $\Phi(1, 3) \rightarrow \{4, -4\})$. If we assume that our calculation of ϕ up to $\phi(3)$ is accurate, then we should expect that the correct value of $\phi(n = 4)$ is contained in *both* pairs. Examining the intersection of $(4, -4)$ and $(4, -16)$, we may infer that $\phi(4) = 4$.

Similarly, we may determine the correct value and sign of $\phi(5)$ via two constraints from $|\Phi|$.

$$\phi(5) = \pm\Phi(2,3) + \phi(2) + \phi(3) = \pm 6 + -4 \rightarrow \{2, -10\} \tag{21}$$

$$\phi(5) = \pm\Phi(1,4) + \phi(1) + \phi(4) = \pm 3 + 5 \rightarrow \{8, 2\} \tag{22}$$

Again, the intersection of the pairs of possible solutions gives the correct answer $\phi(5) = 2$.

The last entry requires finding the intersection among three pairs since there are three non-redundant pieces of data in $|\Phi|$ we may use.

$$\phi(6) = \pm\Phi(3,3) + \phi(3) + \phi(3) = \pm 9 - 2 \rightarrow \{7, -11\} \tag{23}$$

$$\phi(6) = \pm\Phi(2,4) + \phi(2) + \phi(4) = \pm 6 + 1 \rightarrow \{7, -5\} \tag{24}$$

$$\phi(6) = \pm\Phi(1,5) + \phi(1) + \phi(2) = \pm 4 + 3 \rightarrow \{7, -1\} \tag{25}$$

The intersection of the three pairs leads us to conclude that $\phi(6) = 7$.

3.2. Numerical algorithm

In practice, the intersection of solution pairs is never exact and a numerical estimation subject to input noise is required. We devised an algorithm to accurately find the intersection of all pairs of possible solutions. For each $\vec{u} = \vec{m} + \vec{n}$ there are, in general, multiple sets of $(\vec{m}, \vec{n})$ positions with previously calculated phases. Each of these sets generates a pair of solutions for the two signs of $\Phi(\vec{m}, \vec{n})$, say $\theta_{+,i}$ and $\theta_{-,i}$. As seen in the example above, for every i, one of these two values is approximately the same (mod 2π).

Optics EXPRESS

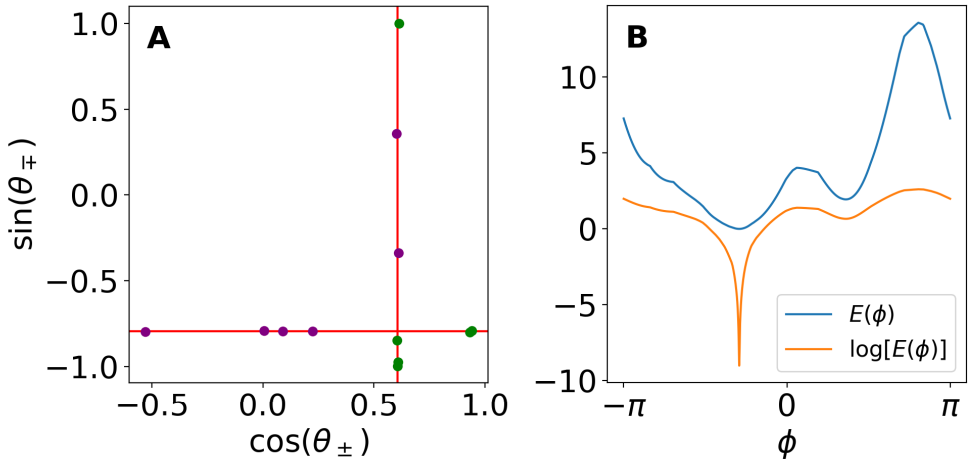

Fig. 3. Successful minimization of an example error function $\log E(\phi)$ in (B) finds the correct intersection of the set of $\theta_\pm$ in figure (A). Points in green are the ordered pairs $(\cos\theta_+, \sin\theta_-)$ while points in purple are the ordered pairs $(\cos\theta_-, \sin\theta_+)$, as described in the main text.

A visually instructive way to determine this common value is to plot each of these pairs as points in a two-dimensional plane, both as (θ_+, θ_-) and (θ_-, θ_+). Thus, either the horizontal and vertical components of each point are common with all the others. Graphically, this means that the points (approximately) form a vertical and horizontal line intersecting at the true solution $(\phi(\vec{u}), \phi(\vec{u}))$. In order to stay in a bounded domain, it is simpler to consider ordered pairs $(\cos(\theta_+), \sin(\theta_-))$ and $(\cos(\theta_-), \sin(\theta_+))$ to constrain the search to $\phi \in [-\pi, \pi]$ and remove 2π offsets of the value of $\theta_\pm$ (see Fig. 3(A)). Finding the intersection given some noise in the data $\theta_\pm$ then amounts to the minimization of the error function

$$E(\phi) = \sum_i \min\left[(\cos(\theta_\pm)_i - \cos(\phi))^2, (\sin(\theta_\mp)_i - \sin(\phi))^2\right] \tag{26}$$

where the sum is over the N pairs of possible solutions for our chosen $\vec{u}$. The optimal value is the desired value of ϕ at $\vec{u}$, $\phi(\vec{u}) = \phi_{\text{opt}}$.

The landscape of the error function $E(\phi)$ presents challenges for conjugate gradient optimization because it contains multiple local minima separated by large barriers. An example for a random pixel in a 2D phase array is shown in Fig. 3(B). Since the value of the phase needs to be optimized for each pixel on the detector, a rapid and accurate method of determining the absolute minimum is desired. This is most straightforwardly accomplished by supplying an optimization algorithm with the minimum value of $\log E(\phi)$ on a grid in $[-\pi, \pi]$; the logarithm increases the contrast of the absolute minima significantly, allowing accurate calculation of an initial guess for the conjugate gradient optimizer. The optimizer polishes the brute-force search to a precise final value.

Since the value of $\phi(\vec{m} + \vec{n})$ depends on previous values of $\phi(\vec{m})$ and $\phi(\vec{n})$, it is especially important that values calculated early in the retrieval are accurate. Depending on the quality of the data in $\Phi(\vec{m}, \vec{n})$, the error function may present multiple deep local minima which cause the algorithm to, initially, choose an incorrect value of ϕ. In this case, $\log[E(\phi)]$ for subsequent pixels in the retrieval sharply increases, indicating that at least one previous pixel has ϕ assigned incorrectly. Plotting the total fit error for all pixels indicates the location of problematic pixels which require resolving by toggling candidate phase values until the total error of all pixels is

Optics EXPRESS

minimized. The consequences of toggling alternate values of ϕ near the origin to minimize the error across all pixels are illustrated nicely in Fig. 4 by comparing the boxed and unboxed figures.

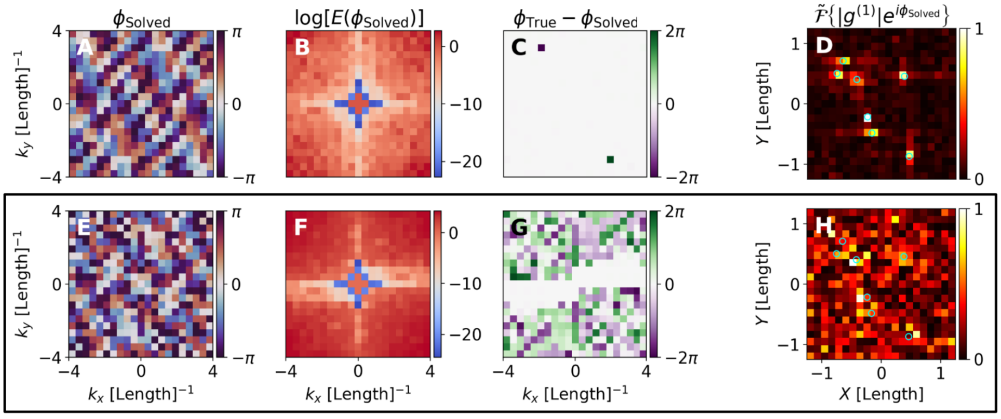

Fig. 4. Exact ab initio phase retrieval from triple correlations both with (A-D) and without (boxed, E-H) alternate value toggling. (A) shows the phase retrieved from the third-order correlations used to produce the object image via Fourier inversion in (D). The true positions of the atoms used in the simulation are indicated by light blue circles in (D) and (H). (B) shows the error values calculated for each pixel during phase retrieval and (C) shows the difference between the true and retrieved phase values. (E-H) shows the same plots for the same set of atoms and number of shots but without alternate phase value toggling. When alternate phase values at pixels adjacent to spikes in the error function are toggled correctly as in (B), the error is reduced and the difference between the retrieved and true values is small. When alternates are not toggled correctly as in (F), the error is large and faithful structure retrieval is less likely. Phase information past the physical edge of the detector ($\left|\vec{k}_{\text{max}}\right| = 2$ in this example) is retrieved via the triple correlations, enhancing real space resolution that would be measured in a typical diffraction experiment.

4. Results

Using Eq. (11) and the algorithm described in Section 3, we can calculate the Fourier phase from triple correlation data and compare the result to the true value. Figure 4 shows the results of phase retrieval in a simulation with a 2D pixel detector. Note that in regions where the error Fig. 4(B) is small, the solved phase matches the true phase quite well. In this example, sufficient phase information is retrieved to fully resolve the seven simulated atoms (blue circles in Fig. 4(D)) with only 10^4 shots. The Fourier inversion was performed using the phase retrieved via our algorithm from the third-order correlation function and $\left|g^{(1)}\right|$ calculated via the second-order correlation function. No use of coherent diffraction data was required.

Acquiring additional shots significantly improves the fidelity of phase retrieval. The primary practical limit on phase retrieval via the triple correlations is the computation of the bispectrum which, for a 2D detector, requires storage of a $(N_{\text{pix}} \times N_{\text{pix}})^2$ floating point array. For large detectors, the bispectrum can rapidly consume all available memory on small workstations. The 11×11 detector simulated in Fig. 4 with 10^4 shots was chosen as a reasonable compromise between memory usage, execution time, and visual impact for this demonstration on a 2015 MacBook Pro running a 2.8GHz Intel i7 processor.

Optics EXPRESS

5. Conclusions

We have described a mathematical solution to the sign problem in phase retrieval from triple correlations of fluorescent or thermal light. We provided a numerical demonstration of our method with simulated data which accurately retrieved the reciprocal space Fourier phase of an atom array. We envision this method as another potential solution to the phase problem in crystallography via photon correlations of fluorescence radiation from atoms pumped by x-ray free-electron lasers. The method presented in this paper may also prove interesting for pulse metrology [32–35], observing many-body correlations in ultracold atomic gases [36–38], imaging in turbid media [39–41], and for imaging with radio telescope arrays [12–14].

Funding. Deutsche Forschungsgemeinschaft (EXC 2056-390715994, 491245950); Deutsches Elektronen-Synchrotron; MIT International Science and Technology Initiatives (MISTI); Hertz Foundation.

Acknowledgments. NP thanks Anlong Chua for helpful discussions regarding Eq. (26) and Fabian Trost for helpful discussions regarding computation of the bispectrum.

Disclosures. The authors declare no conflicts of interest.

Data availability. The data and source code which support the results in this paper are available on Github [42].

Supplemental document. See Supplement 1 for supporting content.

References

1. Y. Shechtman, Y. C. Eldar, O. Cohen, H. N. Chapman, J. Miao, and M. Segev, "Phase retrieval with application to optical imaging: A contemporary overview," IEEE Signal Process. Mag. **32**(3), 87–109 (2015).
2. J. W. Goodman, *Introduction to Fourier Optics* (McGraw-Hill, 2003), 2nd ed.
3. R. Hanbury Brown, "A test of a new type of stellar interferometer on sirius," Nature **178**(4541), 1046–1048 (1956).
4. A. Classen, K. Ayyer, H. N. Chapman, R. Röhlsberger, and J. von Zanthier, "Incoherent diffractive imaging via intensity correlations of hard x-rays," Phys. Rev. Lett. **119**(5), 053401 (2017).
5. R. Schneider, T. Mehringer, and G. Mercurio, *et al.*, "Quantum imaging with incoherently scattered light from a free-electron laser," Nat. Phys. **14**(2), 126–129 (2018).
6. F. Trost, K. Ayyer, and H. N. Chapman, "Photon statistics and signal to noise ratio for incoherent diffraction imaging," New J. Phys. **22**(8), 083070 (2020).
7. P. J. Ho, C. Knight, and L. Young, "Fluorescence intensity correlation imaging with high spatial resolution and elemental contrast using intense x-ray pulses," Struct. Dyn. **8**(4), 044101 (2021).
8. L. M. Lohse, M. Vassholz, and T. Salditt, "On incoherent diffractive imaging," Acta Crystallogr. Sect. A Foundations Adv. **77**(5), 480–496 (2021).
9. F. Trost, K. Ayyer, and M. Prasciolu, *et al.*, "Imaging via correlation of X-ray fluorescence photons," Phys. Rev. Lett. **130**(17), 173201 (2023).
10. R. Twiss, "Applications of intensity interferometry in physics and astronomy," Opt. Acta: Int. J. Opt. **16**(4), 423–451 (1969).
11. H. Gamo, "Triple correlator of photoelectric fluctuations as a spectroscopic tool," J. Appl. Phys. **34**(4), 875–876 (1963).
12. P. D. Nuñez and A. Domiciano de Souza, "Capabilities of future intensity interferometers for observing fast-rotating stars: imaging with two- and three-telescope correlations," Mon. Not. R. Astron. Soc. **453**(2), 1999–2005 (2015).
13. T. Wentz and P. Saha, "Feasibility of observing Hanbury Brown and Twiss phase," Mon. Not. R. Astron. Soc. **446**(2), 2065–2072 (2014).
14. D. Dravins, T. Lagadec, and P. D. Nuñez, "Long-baseline optical intensity interferometry: Laboratory demonstration of diffraction-limited imaging," Astron. & Astrophys. **580**, A99 (2015).
15. V. Malvimat, O. Wucknitz, and P. Saha, "Intensity interferometry with more than two detectors?" Mon. Not. R. Astron. Soc. **437**(1), 798–803 (2014).
16. D. Dravins, S. LeBohec, H. Jensen, and P. D. Nuñez, "Optical intensity interferometry with the Cherenkov telescope array," Astropart. Phys. **43**, 331–347 (2013).
17. T. Sato, S. Wadaka, J. Yamamoto, and J. Ishii, "Imaging system using an intensity triple correlator," Appl. Opt. **17**(13), 2047 (1978).
18. T. Sato, J. Ishii, and S. Wadaka, "Computer controlled image sensor and its application," Appl. Opt. **18**(4), 485 (1979).
19. T. Sato, K. Sasaki, and K. Ando, "Adaptive techniques for precise detection of the coherence function by an intensity triple correlator," Appl. Opt. **20**(12), 2055 (1981).
20. P. Fontana, "Multidetector intensity interferometers," J. Appl. Phys. **54**(2), 473–480 (1983).
21. A. W. Lohmann, G. Weigelt, and B. Wirnitzer, "Speckle masking in astronomy: triple correlation theory and applications," Appl. Opt. **22**(24), 4028 (1983).
22. A. W. Lohmann and B. Wirnitzer, "Triple correlations," Proc. IEEE **72**(7), 889–901 (1984).

Optics EXPRESS

23. H. Bartelt, A. W. Lohmann, and B. Wirnitzer, "Phase and amplitude recovery from bispectra," Appl. Opt. **23**(18), 3121 (1984).
24. T. Matsuoka and T. Ulrych, "Phase estimation using the bispectrum," Proc. IEEE **72**(10), 1403–1411 (1984).
25. J. E. Baldwin, C. A. Haniff, C. D. Mackay, and P. J. Warner, "Closure phase in high-resolution optical imaging," Nature **320**(6063), 595–597 (1986).
26. J. I. Yellott and G. J. Iverson, "Uniqueness properties of higher-order autocorrelation functions," J. Opt. Soc. Am. A **9**(3), 388 (1992).
27. A. S. Marathay, Y. Hu, and L. Shao, "Phase function of spatial coherence from second-, third-, and fourth- order intensity correlations," Opt. Eng. **33**(10), 3265 (1994).
28. E. Sayrol, C. Nikias, and A. Gasull, "Image restoration using the w-slice method," IEEE Trans. on Image Process. **4**(8), 1174–1181 (1995).
29. R. Holambe, A. Ray, and T. Basu, "Signal phase recovery using the bispectrum," Signal Process. **55**(3), 321–337 (1996).
30. G. Shoulga and E. N. Ribak, "Toward spectral intensity interferometry," Appl. Opt. **56**(1), A23 (2017).
31. R. Loudon, *The Quantum Theory of Light* (Oxford University Press, 2000), 3rd ed.
32. T. Feurer, S. Niedermeier, and R. Sauerbrey, "Measuring the temporal intensity of ultrashort laser pulses by triple correlation," Appl. Phys. B: Lasers Opt. **66**(2), 163–168 (1998).
33. T.-M. Liu, Y.-C. Huang, G.-W. Chern, K.-H. Lin, C.-J. Lee, Y.-C. Hung, and C.-K. Sun, "Triple-optical autocorrelation for direct optical pulse-shape measurement," Appl. Phys. Lett. **81**(8), 1402–1404 (2002).
34. I. Inoue, K. Tamasaku, T. Osaka, Y. Inubushi, and M. Yabashi, "Determination of x-ray pulse duration via intensity correlation measurements of x-ray fluorescence," J. Synchrotron Radiat. **26**(6), 2050–2054 (2019).
35. N. Nakamura, S. Matsuyama, T. Inoue, I. Inoue, J. Yamada, T. Osaka, M. Yabashi, T. Ishikawa, and K. Yamauchi, "Focus characterization of an x-ray free-electron laser by intensity correlation measurement of x-ray fluorescence," J. Synchrotron Radiat. **27**(5), 1366–1371 (2020).
36. S. Fölling, F. Gerbier, A. Widera, O. Mandel, T. Gericke, and I. Bloch, "Spatial quantum noise interferometry in expanding ultracold atom clouds," Nature **434**(7032), 481–484 (2005).
37. T. Jeltes, J. M. McNamara, W. Hogervorst, W. Vassen, V. Krachmalnicoff, M. Schellekens, A. Perrin, H. Chang, D. Boiron, A. Aspect, and C. I. Westbrook, "Comparison of the Hanbury Brown–Twiss effect for bosons and fermions," Nature **445**(7126), 402–405 (2007).
38. M. R. Andrews, C. Townsend, H. Miesner, D. Durfee, D. Kurn, and W. Ketterle, "Observation of interference between two bose condensates," Science **275**(5300), 637–641 (1997).
39. J. Bertolotti, E. G. van Putten, C. Blum, A. Lagendijk, W. L. Vos, and A. P. Mosk, "Non-invasive imaging through opaque scattering layers," Nature **491**(7423), 232–234 (2012).
40. O. Katz, P. Heidmann, M. Fink, and S. Gigan, "Non-invasive single-shot imaging through scattering layers and around corners via speckle correlations," Nat. Photonics **8**(10), 784–790 (2014).
41. G. Stern and O. Katz, "Non-invasive focusing through scattering layers using speckle-correlations," Opt. Lett. **44**(1), 143–146 (2019).
42. N. Peard and K. Ayyer, "CorrSpeck," Github (2022), https://github.com/npeard/CorrSpeck.